Characterization of a low pressure supersonic plasma jet

S Caldirola[1], R Barni[1] and C Riccardi[1]

[1] Dipartimento di Fisica G. Occhialini, Università degli Studi di Milano-Bicocca, piazza della Scienza 3, I-20126 Milano, Italy

E-mail: claudia.riccardi@mib.infn.it

Abstract. Plasma assisted supersonic jet deposition (PA-SJD) is a technique which combines a inductively coupled plasma (ICP) with a supersonic jet for the fabrication of thin films having a desired morphology. A reactive argon-oxygen plasma is employed to dissociate an organic precursor (titanium tetra-isopropoxide for TiO_2 thin films) in a first vacuum chamber which is connected through a nozzle to a lower pressure chamber. The pressure difference produces a supersonic jet, seeded with nanoparticles. Along the jet the nucleation and aggregation of nanoparticles can be controlled to obtain nanostructured depositions. We report here the results of an analysis performed with a quadrupole mass spectrometer (QMS) which was used to sample neutrals and ions from the jet at different positions along the centerline of the supersonic expansion.

1. Introduction

Thin films made of titanium dioxide have been widely used for different applications in a great number of research areas: TiO_2 is biologically and chemically inert, it combines a high dielectric constant with high refractive index and exhibits a wide-bandgap. These properties make it well suited for microelectronic and semiconductors applications, for sensors, ultraviolet filters and antireflection coating, photocatalysts and photovoltaic [1-5]. The growth of thin and ultra-thin films of TiO_2 may be achieved using a large variety of techniques such as chemical vapour deposition (CVD), RF sputtering, pulsed laser deposition (PLD) or plasma enhanced CVD (PECVD). Film morphology and structure can greatly enhance the physical properties of thin films. The growth process used determines the structure; different techniques can be adopted, depending on which properties are to enhance in the film [6-9]. Modelling the nanoparticles which create and assemble the film it is possible to achieve very promising results, although it requires a bottom-up approach capable of tailoring the properties with a high level of control or a complex set-up. [10,11]. Unfortunately there is no deposition procedure which can easily achieve an accurate control on both the chemical composition and the nanostructure of a thin film and that can be considered truly versatile or up-scalable. In order to model the film growth and its morphology we proposed an innovative approach to thin films deposition which we named Plasma Assisted Supersonic Jet Deposition (PA-SJD) [12]. An inductively coupled plasma source (ICP) is used to generate a high density argon-oxygen plasma at low pressure inside a cylindrical vacuum chamber which is connected through a converging nozzle to a lower pressure chamber. The pressure ratio between the two chambers determines and characterizes the formation of a supersonic expanding jet. PA-SJD technique was already employed using an


Content from this work may be used under the terms of the Creative Commons Attribution 3.0 licence. Any further distribution of this work must maintain attribution to the author(s) and the title of the work, journal citation and DOI.
Published under licence by IOP Publishing Ltd

organic precursor of titanium for TiO_2 nanostructured thin film depositions [13]. A vaporizer injects the precursor inside the ICP chamber where the reactive plasma dissociates the chemical bonds. The dissociated precursor then flows in the deposition chamber with the expanding jet: the light gas carrier mixture accelerates different titanium nanoparticles up to 0.05-0.3 eV. As the gas expands, pressure, temperature and density decrease creating an energetic and low-collisional flow. In this way the deposition process is divided in two different and tunable steps: the production of the TiO_x seeds and their acceleration and assembly on a substrate. A detailed understanding of the gas expansion is fundamental in order of being able to control the growth and the morphology for nanostructured depositions which are closely related to the nanoparticles energy and diameter. In this work we show the results obtained from a deep characterization of the supersonic jet with a movable quadrupole mass spectrometer (QMS) able to sample neutral gas, radicals and ions at different distances from the nozzle along the axis of symmetry of the gas expansion. Plasma properties were simultaneously measured by optical emission spectroscopy (OES) observing the emission spectra from atoms, molecules and ions present in the plasma chamber and electrical diagnostic, acquiring time series of voltage and current flowing through the radiofrequency antenna of the ICP.

2. Experimental set-up

In this section we will describe the layout of the experimental set-up, sketched in figure 1, and the diagnostics employed.

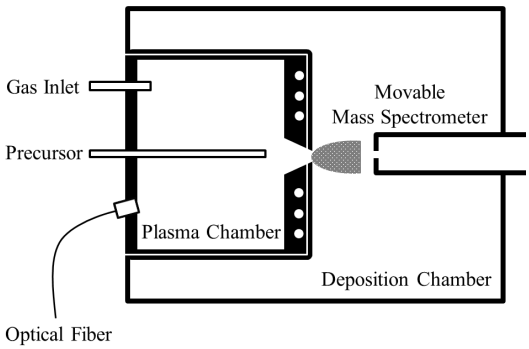

Figure 1. Experimental set-up.

2.1. Vacuum vessel

PA-SJD is a two step deposition process which take place in two stainless-steel cylindrical vacuum vessels connected through a nozzle: the plasma chamber (95 mm long with 62.5 mm radius) and the deposition chamber (200 mm long with 160 mm for inner radius). On the bottom of the deposition chamber a circular conductance (100 mm diameter sized, variable by closing a gate valve) connects our vessel to the main pumping group: a turbo molecular and a rotary pump. On the right side of the chamber there is also an aperture which put the system in connection with the quadrupole mass spectrometer, which can sample the gas from a little conductance (a 0.1 mm diameter circular orifice). A turbo molecular and a rotary pump preserve the purity of the spectrometry measurements keeping the instrument below 10^{-4} Pa. The left lid of the biggest vacuum chamber is in direct contact with the plasma chamber and it contains the inlets for the gas and the precursor. The gas is injected from two different mass-flow controllers, the first ranging from 1.4 to 14 sccm for Ar, the second from 5 to 50 sccm for O_2. The lid also has

two connections to the inductive antenna (planar copper coil cooled by deionized water) and a quartz window to monitor the discharges and acquire optical emission spectra. The deposition chamber is connected with the plasma chamber through a rectangular converging nozzle. The exit area of the nozzle is a circular hole with a diameter of 6.9 mm. The pressure in the chambers and the spectrometer is monitored using three capacitance pressure gauges. The pressure ratio $R = p_P/p_D$ between the two chambers can be varied by closing the gate valve which connects the main pumping group from 40 to 1 to model the supersonic jet geometry and energy.

2.2. ICP source

An ICP can provide plasma densities between 10^{11} and 10^{13} cm^{-3} with an excellent uniformity of the plasma over diameters of at least 20 cm, and low, controllable ion energies [14]. In addition to this it ensures low contamination by sputtering products from the reactor walls. Inside the plasma chamber an inductively coupled plasma is generated by a 13.56 MHz radiofrequency power generator (Huttinger PFG 1600 RF). The generator is connected through a tunable matching box (L-type) to a two and three quarters loop planar antenna made of copper wire (having a measured inductance of 2.5 μH and an impedance of 213 Ω at RF [12]) located on the right side of the plasma chamber, inside a teflon scaffold covered by an alumina disc to reduce teflon sputtering. All the vessel is grounded at the same reference potential.

2.3. TTIP precursor

Titanium precursor can be introduced inside the first chamber when the plasma discharge is sustained at a sufficiently high power level. TiO_2 films can be obtained from different organic precursors, titanium alkoxide are preferable such as $Ti(OPr^i)_4$, which already display the TiO_4 tetrahedral motif of titanium dioxide lattice in their chemical structure [15]. In this work we chose titanium (IV) Tetraisopropoxide $Ti(OCH(CH_3)_2)_4$ or TTIP, which is liquid at 20°C and it is heated with a power transformer to reach the vapour phase. The temperature can be monitored with a thermocouple over the precursor tank and varied to obtain different precursor flows (from 0.25 to 0.75 grams per hour). Operating at temperatures between 40 and 47°C the vapour pressure of TTIP is sufficiently high to create a stable flow inside the plasma chamber.

2.4. Diagnostics

During each plasma discharge, the electrical parameters were observed measuring times series of voltage and current at the two different side of the planar antenna. The voltage directly exiting the matching box was measured using a high-voltage probe (Tektronix P6015A), while the current flowing in the antenna was acquired with a Rogowski probe positioned at the grounded side of the coil. Both signals were simultaneously acquired using a digital oscilloscope at 4 GHz sampling frequency to obtain a detailed electrical characterization.

Optical emission spectroscopy (OES) is a well know non-intrusive diagnostics which has already been applied in many plasma discharges [16,17]. Revealing the light emitted from atoms, molecules and ions which are excited from free electrons in the discharge, it is possible to understand the main reaction processes in the plasma. The intensity of emission lines can identify chemical species and allows to gain insight about their abundances. From the quartz window facing the plasma chamber optical emission spectra (OES) were acquired using two different low resolution spectrometers, as already described in our previous works [12,16].

Quadrupole mass spectrometers can provide an in situ, real time sensing diagnostic for many different applications. We employed a particular QMS (Hiden EQP-1000 Analyser) well suited for plasma analysis: neutrals, radicals and ion species can be detected providing precious information on our system [18]. The QMS is movable on a sliding support, thus capable of performing mass or energy scan along the centerline of the main vacuum vessel, also reaching the nozzle which connects the two chambers. In our set-up the chemical species sampled from

the instrument are reasonably the same involved in the depositions. The gas exiting from the plasma chamber is sampled by a small orifice (100 μm of diameter) into the QMS. This instrument consist of an electron-impact ionization region, an optic system for ion focusing, an high transmission 45° sector field ion energy analyser and a quadrupole mass spectrometer. It is capable of measuring mass and energy spectra allowing detailed analysis of the plasma. When activated, the ionization of neutral species is obtained by an electron-impact source: a oxide coated iridium filament emits thermal electrons which are accelerated toward a grid at a determined energy. In this process, some molecules can be ionized twice or fragmented into lighter species thus measured mass spectra can be affected by characteristic fragmentation patterns. When the ionization is not activated, the ions measured are those produced outside the QMS. The detector is a secondary electron multiplier pulse-counting detector which can provide mass spectra in counts/sec over m/z from 0 up to 1000 amu and energy spectra in counts/sec over eV from -100 to 100 eV. Trends in intensity may also be measured and plotted against time for a short list of relevant masses providing a truly real time, quick and direct measurement.

3. Results and discussion

The QMS was the main diagnostic used to collect data and it was employed to characterize the formation of the supersonic jet seeded with nanoparticles reproducing the experimental conditions already optimized and adopted for thin film depositions [12]. The gas fluxes in the plasma chamber are first set in order to reach a pressure of about 10 Pa with a 2:3 mixture of Ar and O_2. A high concentration of oxygen is fundamental inside the plasma chamber to properly dissociate the precursor, anyway argon gas is also important to create a stable plasma without the requirements of an excessively high power input. The pressure in the deposition chamber can be adjusted to set a desired pressure ratio R. A ICP plasma is generated increasing the power flowing into the planar coil and regulating at each step the L-type matching network to ensure the maximum power transfer. For power values below 175 W the plasma appears in a dim and low density state where the coupling between the antenna and the plasma is just partial, the so called E-mode. As the power increases, a clear transition happens upon reaching the H-mode in which the coupling is fully inductive and the main ionization mechanism which sustains the plasma is the power cession between the current flowing inside the coil and the plasma itself. At 450 W the plasma is stable and the discharge is purely inductive thus it is possible to inject the precursor by adjusting the temperature of the titanium isopropoxide (TTIP) tank and opening a micrometer valve. With the diagnostic system discussed above, we investigated the supersonic jet inside our deposition chamber, characterized the plasma conditions and observed the fragmentation of a TTIP precursor from the plasma directly sampling neutrals, radicals and ions along the jet.

3.1. Formation of the supersonic jet

Under-expanded jet are used in many applications as an effective tool for the the creation of a molecular beam or as nanoparticle source. Compared to effusive beams, such as those used in molecular beam epitaxy, supersonic beams provide higher intensity and directionality allowing deposition with very high growth rates. When a heavy specie is diluted in a lighter gas there is the formation of a seeded supersonic beam. Seeded supersonic beams are extensively used to cool and to accelerate heavy species such as nanoparticles [19,20]. The rapid and unconfined expansion of a gas exiting from a sonic orifice into a low pressure chamber creates a supersonic and directed jet. As the volume increases, temperature, pressure and density abruptly decrease according to the laws which describe an isentropic process, thus accelerating the gas particles increasing the Mach number (defined as the ratio between the velocity of a particle and the local sound speed) above 1. The thermal energy of the molecules is converted into flow velocity forming the supersonic jet. The expansion ends with a normal shock, called Mach disc, where

temperature, pressure and density reach the background values while the Mach number returns below 1. The properties of this supersonic beam are mainly determined by the size and shape of the nozzle and by the thermodynamic properties of the gas upstream of the nozzle [21,22]. A schematic representation of the geometry of a supersonic jet is sketched in figure 2.

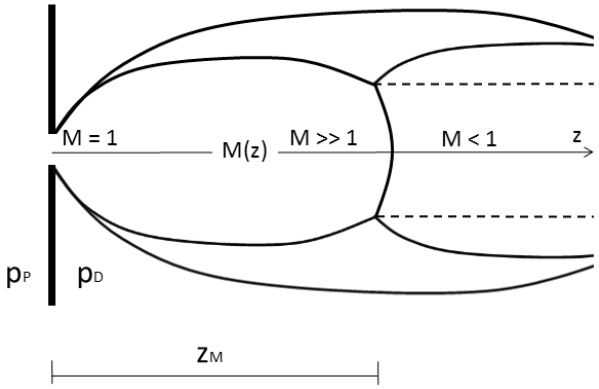

Figure 2. Schematic representation of the gas expansion between the plasma chamber and the deposition chamber. The Mach number (M) variations and the Mach disc position z_M are indicated.

Some useful empirical equations, verified experimentally, can help to reconstruct with good accuracy the geometry of the supersonic jet, as for the Mach disc distance from the nozzle z_M we find from [23]:

$$\frac{z_M}{D_n} = 0.67\sqrt{R} \tag{1}$$

This law does not depend on the gas adiabatic index γ, but only on the exit area of the nozzle (in particular on its diameter D_n for a circular orifice) and on the ratio R between the pressure in the upstream chamber and the pressure downstream. In our experimental works we used a converging nozzle followed by a circular orifice. The converging nozzle (a rounded rectangle which area decreases of about an half in 15 mm length from its initial value of 22x60 mm) ensure a sonic flow at the exit: Mach number is equal to 1, pressure and density values about 0.5 and 0.6 times the upstream values (depending on the γ of the gas). This favours the formation of the jet, even if it is not fundamental as described in [24]. The exit area of our nozzle is a circular orifice having 6.9 mm of diameter, using the equation above assuming that our values for $R = p_P/p_D$ range from 40 to 2, we obtain a Mach disc position varying from 29 to 6.5 mm, depending on the background pressure we set in the deposition chamber. From [23] it is also possible to obtain some empirical equations describing the variation of Mach number and pressure along the centerline of the expansion, as a function of the position z and we estimate Mach numbers up to 8 or 3 respectively for z about 29 or 6.5 mm. We derived an equation for the variation of density along the jet combining the equation proposed in [25] for the pressure on a flat plate positioned at a certain z with the isentropic relations for an ideal gas, obtaining:

$$\frac{n(z)}{n_{Plasma}} = \left(1.44\left(\frac{z}{D_n}\right)^2 - 0.65\frac{z}{D_n} + 0.87\right)^{-1/\gamma} \tag{2}$$

With the movable QMS it was possible to acquire mass spectra along the supersonic jet, measuring a signal proportional to the local density at the entrance of the instrument. Bow

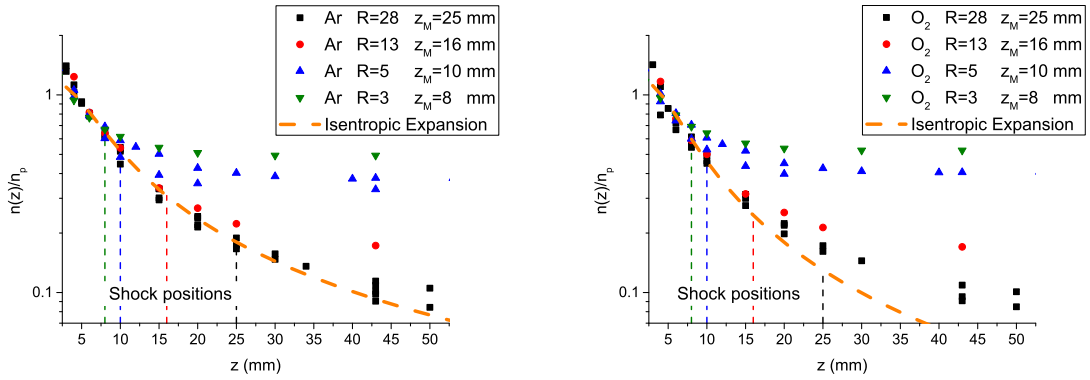

Figure 3. QMS data acquired for argon atoms (left) and oxygen molecules (right) in the argon-oxygen mixture used in the experiments for different pressure ratios R. This implies a different position for the Mach disc z_M which determines the end of the supersonic jet. Coloured vertical bars indicate different z_M.

shock effects are known to perturb or affect the supersonic jet when an obstacle, such as the substrate, is placed at a certain position [26]. By measuring with this experimental set-up we can have a reliable value of the jet structure and composition during a deposition. Our data, stored as counts per second for different m/z ratios, was then renormalized to reproduce the density ratio which appears in the equation above. Statistical errors are generally small (about 1 %) when the plasma is turned off, a set of measurements was taken acquiring the full mass spectra and integrating the area of the peaks, another was acquired directly measuring each second the values of some chosen mass. Each measure performed during the same experiment shows a good reproducibility, unfortunately systematic errors make it difficult to exactly reproduce the same pressure conditions (and also temperature when the plasma is generated) during a different experiment. The agreement with the isentropic expansion law inside the jet given above is very good especially for Ar, as seen in figure 3. Each series of data correspond to a different pressure ratio obtained at fixed pressure in the plasma chamber p_P (about 8 Pa) and changing the background pressure p_D from 0.2 to 4 Pa. For all these values the mean free path in the deposition chamber of the gas is of the order of magnitude of 10 mm, thus we don't expect a steep gradient or an abrupt shock at the end of the supersonic jet. A higher R implies greater distances of the Mach disc from the nozzle z_M, our data show fairly well that the density follows the expected isentropic expansion equation until z_M. After this point the density resets slowly reaching the background values of the deposition chamber.

3.2. Plasma analysis

The results obtained with the free gas jet were then observed and studied when the plasma is created in the first chamber. The generation of the inductive plasma increases pressure and temperature in the plasma chamber, usually from 8 to 10 Pa. Higher temperature and pressure cause higher density and kinetic energy in the supersonic jet, corresponding to a higher flow speed and small differences in the pressure ratio. During each plasma discharge time series of voltage and current across the antenna were acquired with a digital oscilloscope. Increasing the power output from the generator a sharp transition between the E and the H-mode takes place about 175 W.

This transition is shown in the graph on the left in figure 4 where the root mean square values of the voltage drop across the coil and the current flowing through are reported. We also measured emission spectra with different spectrometers and optical fibers (described in the

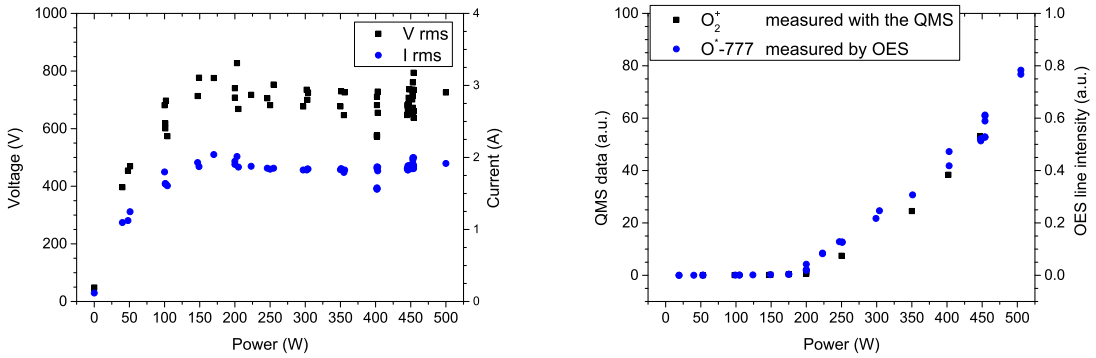

Figure 4. Electrical discharge data show a clear transition increasing the power input (graph on the left). When the fully inductive coupling is reached (H-mode) there is a net increases in plasma density, which was measured both with the QMS and by OES (graph on the right).

experimental set-up section) directly in the first chamber during each plasma discharge. The line emission from the atoms in the plasma, dark subtracted and corrected by the sensitivity of the instruments, can be used to retrieve informations on the radical concentration or on the plasma parameters (electron temperature and density). A detailed OES analysis is far from the purposes of this article, anyway an insight on the main reactive species in the plasma chamber can be gained from figure 6 where a typical spectra is plotted. The most intense lines in the Ar-O_2 plasma spectra are generated from de-excitations of the argon states $3p^5 4p \rightarrow 3p^5 4s$ (wavelength from 415 to 433 nm) and $3p^5 5p \rightarrow 3p^5 4s$ (wavelength from 697 up to 812 nm). Also atomic oxygen lines at 777 and 845 nm are well distinguishable, corresponding to the following de-excitation: $2p^3 3p \rightarrow 2p^3 3s$. Assuming that the electron temperature variations are low at different powers (as seen in [12]), the light emission of the plasma is mostly dependant on the plasma charge density and the initial concentration of emitting atoms. Figure 4 also shows on a separated graph the variation of O_2 ion density, measured with the QMS far from the jet at 100 mm, and of the line 777 obtained simultaneously from the OES. The increase is similar for both the diagnostics, there is a significant increase of ion density after the transition to the H-mode.

The distribution of species along the jet was studied at 450 W, 10 Pa of pressure in the plasma chamber and 0.34 Pa in the deposition chamber, with the 2:3 argon-oxygen mixture. Neutrals and ions scans were performed, and we report a typical variation of QMS counts along the z axis in figure 5. The neutrals measured in the jet are consistent with the data collected without the plasma, although the shock seems stronger and the gas quickly reaches the background values. The ion density variation is highly influenced by the shock for both species, as the neutral gas expands isentropically, also the ion density decreases but exhibits a clear maximum just after the shock position. Far from the shock ion signal can still be measured but it appears very low and abruptly decreasing. Ions were collected at a fixed energy value during mass scans, so their values may be a description of the only high energetic population of the spectra (since we tuned the instrument to detect the highly populated peak of their energetic distribution function, at 7 eV). Anyway in similar experiments charge distributions like those shown here were observed [27].

3.3. Precursor injection

Heating the precursor injection system at temperatures about 45 °C we obtained stable TTIP fluxes of approximately 0.48 g per hour inside the plasma chamber. Inside the argon-oxygen plasma, TTIP (m/z = 284) is dissociated mainly by the high-temperature heating, electron

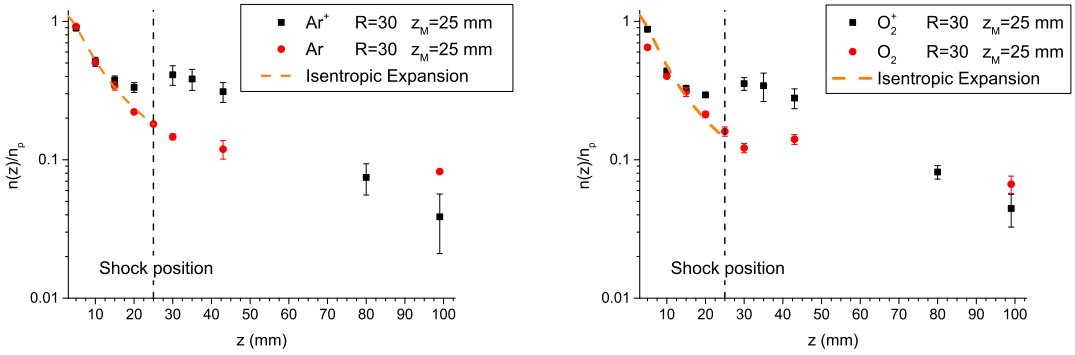

Figure 5. QMS data acquired for neutrals and ions in argon-oxygen plasma. In the graph on the left data for argon are shown, while molecular oxygen is reported on the right. Data have been normalized to reproduce the density variation expected during the supersonic expansion (dashed orange curve). The Mach disc position z_M determines the shock inside the chamber and is indicated with a vertical bar.

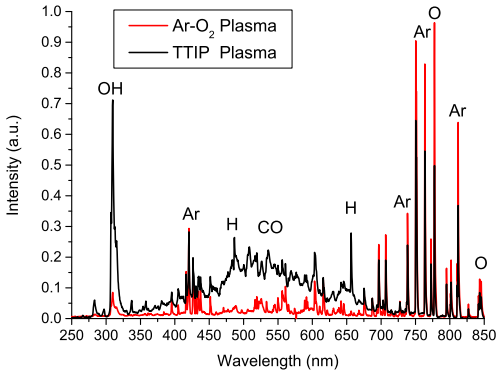

Figure 6. Example of two successively optical emission spectra measured first in a simple argon-oxygen plasma discharge (red line) and then injecting the TTIP precursor (black line).

impact and reactive species, in particular oxygen. The radical oxygen reduction is clearly visible from the emission spectra measured and shown in figure 6. From OES also hydrogen, carbon oxide and hydroxyl radical emission lines can be identified (respectively lines 487 and 565 nm, from 500 to 600 nm, 309 nm). A more complete spectrum of the precursor dissociation was easily measured with the QMS and it is reported in figure 7, in table 1 the identified species are shown (determined from both literature and looking at the titanium isotope ratios [28]).

In the mass range from 300 to 1000 m/z no evidence of other species or nanoparticles was found with this set-up. Inside the supersonic jet, the heavy TTIP products are accelerated from the argon-oxygen mixture at velocities comparable to a fraction of the light gas flow velocity, as a function of their mass and diameter [19]. Again different measurements were performed acquiring neutrals and ions with the QMS reproducing different conditions adopted for thin film depositions. The values for argon and oxygen nicely resemble the results obtained for the simple plasma discussed above.

In figure 8 we see the distribution of some selected species along the jet. The behaviour of

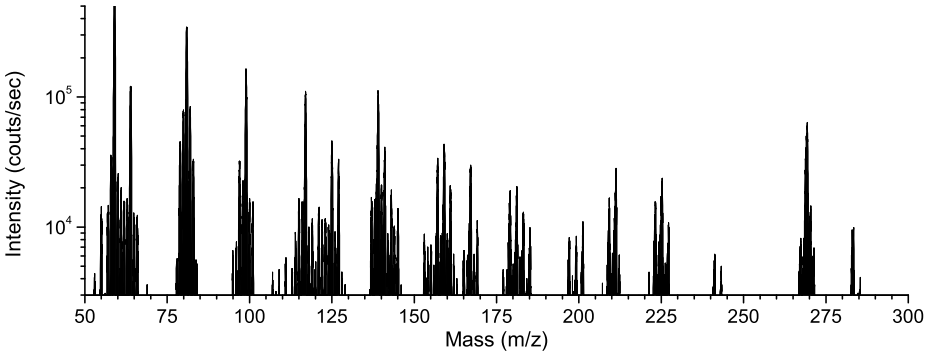

Figure 7. Mass spectra measured at 5 mm of distance from the nozzle during a plasma discharge with TTIP. Electron impact ionization at 70 eV creates different fragments which alter the real chemical composition detected. However most of these peaks have also been measured as ions, so they are originated outside of the QMS and present in the jet, but their sensitivity can not be fully trusted.

Table 1. Main products of the TTIP (m/z=284,$Ti(OCH(CH_3)_2)_4$) dissociation measured during experiments.

m/z	Ion	m/z	Ion
15	CH_3	139	$TiO_2(OCH(CH_3)_2)$
43	$CH(CH_3)_2$	167	$Ti(OCH(CH_3)_2)_2H$
59	$OCH(CH_3)_2$	181	$TiO(OCH(CH_3)_2)_2$-H
64	TiO	211	$Ti(OCH(CH_3)_2)_3H$-CH_3
81	TiO_2H	225	$Ti(OCH(CH_3)_2)_3$
99	TiO_3H_3	243	$Ti(OCH(CH_3)_2)_4$-$CH(CH_3)_2$
125	$TiO(OCH(CH_3)_2)$	269	$Ti(OCH(CH_3)_2)_4$-CH_3

TiO_2H and TiO_3H_3 is very similar to data already shown for argon and oxygen neutral. In the graph on the right it is possible to observe a much different behaviour for higher mass neutrals and ions. This can be due to the different acceleration drag forces and the arise of slip-factors which can cause particles separation along the jet.

4. Conclusions

A characterization of the low pressure supersonic plasma jet employed for thin film depositions was presented. The physics which describes the formation of the jet was reconstructed and verified experimentally by QMS measurements. After a brief description of the main plasma state, measurements along the jet was shown first when the ICP is generated, then when the TTIP precursor is injected. Sampling neutral gas species and ions at different distances from the nozzle it was possible to gain an insight on the precursor dissociation and the components along the supersonic jet which influence our depositions.

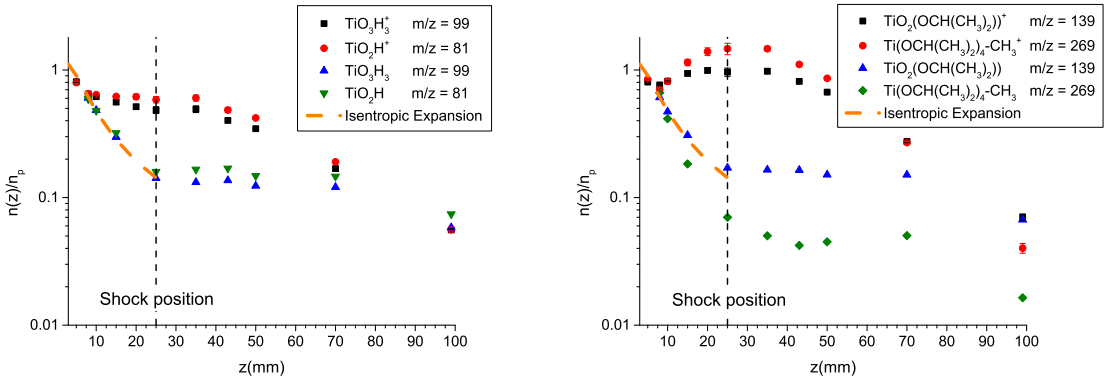

Figure 8. QMS data acquired for neutrals and ions in TTIP reactive plasma. In the graph on the left data for lighter TiO_x seeds are shown, while two heavier masses are reported on the right. Data have been normalized to reproduce the density variation expected during the supersonic expansion (dashed orange curve). The Mach disc position z_M determines the shock inside the chamber and is indicated with a vertical bar.

References

[1] Grant F A 1959 *Rev. Mod. Phys.* **31** 636
[2] Yeung K S 1983 *Thin Solid Films* **109** 169
[3] Kurtz S R, Gordon R G 1987 *Thin Solid Films* **147** 167
[4] Mills A, Le Hunte S 1997 *J. Photochem. Photobiol.* A **108** 1
[5] Fujishima A, Hashimoto K, Watanabe T 1999 *TiO2 Photocatalysis: Fundamentals and Applications* BKC, Tokyo
[6] Chaturvedi S 2011 *J Mater Sci* **46** 3669
[7] R. Messier, A. P. Giri, and R. A. Roy 1984 *J. Vac. Sci. Technol.* A **2** 500
[8] Borras A, Cotrino J, Gonzalez-Elipe A R 2007 *J. Electrochem. Soc.* **154** 152
[9] Dwivedi N, Kumar S, Malik H K 2011 *ACS Appl. Mater. Interfaces* **3** 4268
[10] Milani P, Piseri P,Barborini E, Podesta A, Lenardi C 2001 *J. Vac. Sci. Technol.* A **19** 2025
[11] Dick B, Brett M J, Smy T 2003 *J. Vac. Sci. Technol.* B **21** 2569
[12] Biganzoli I, Fumagalli F, Di Fonzo F, Barni R, Riccardi C 2012 *J. Mod. Phys.* **3**, 1626
[13] Trifiletti V, Ruffo R, Turrini C, Tassetti D, Brescia R, Di Fonzo F, Riccardi C, Abbotto A 2013 *J. Mater. Chem.* A **1**, 11665
[14] Kortshagen U, Zethoff NI, 1995 *Plasma Sources Sci. Technol.* **4**, 541
[15] Nizard H, Kosinova M L, Fainer N I, Rumyantsev M Yu, Ayupov B M, Shubin Yu V, 2008 *Surf. Coat. Technol.* **202**, 4076
[16] Barni R, Zanini S, Riccardi C 2008 *Vacuum* **82** 217
[17] Barni R, Riccardi C, Selli E, Massafra M R, Marcandalli B, Orsini F, Poletti G, Meda L 2005 *Plasma Process. Polym.* **2** 64
[18] Barni R, Zanini S, Riccardi C 2012 *Advances in Physical Chemistry* **2012** 205380
[19] Huang C, Nichols W T, O'Brien D T, Becker M F, Kovar D, Keto J W, 2007 *J. Appl. Phys.* **101**, 064902
[20] Mazza T, Devetta M, Milani P, Bongiorno G,Coreno M, Piseri P 2011 *New J. Phys.* **13** 023009
[21] Fenn J B 2000 *Int. J. Mass Spectrom.* **200** 459
[22] Crist S, Sherman P, Glass D 1966 *AIAA Journal* **4** (1) 68
[23] Ashkenas H, Sherman F 1966 *Rarefied Gasdynamics* **4** Academic Press, New York
[24] Murphy H R, Miller D R 1984 *J. Phys. Chem.* **88** No.20 4474
[25] Abouali O, Saadabadi S, Emdad H 2011 *J. Aerosol Sci.* **42** 65
[26] de la Mora J F 1985 *J. Chem. Phys.* **82** No. 7, 3453
[27] Robin L, Vervisch P, Cheron B G 1994 *Phys. Plasmas* **1** No. 2, 444
[28] Rahtu A, Ritala M 2002 *Chem. Vap. Deposition* **8** No. 1, 21